Science Translational Medicine
AAAS

www.sciencetranslationalmedicine.org/cgi/content/full/8/346/346ra91/DC1

Supplementary Materials for

Robust classification of bacterial and viral infections via integrated host gene expression diagnostics

Timothy E. Sweeney,* Hector R. Wong, Purvesh Khatri*

*Corresponding author. Email: tes17@stanford.edu (T.E.S.); pkhatri@stanford.edu (P.K.)

Published 6 July 2016, *Sci. Transl. Med.* **8**, 346ra91 (2016)
DOI: 10.1126/scitranslmed.aaf7165

The PDF file includes:

Other Supplementary Material for this manuscript includes the following:
(available at www.sciencetranslationalmedicine.org/cgi/content/full/8/346/346ra91/DC1)

Table S4 (.csv format). NanoString data.

A

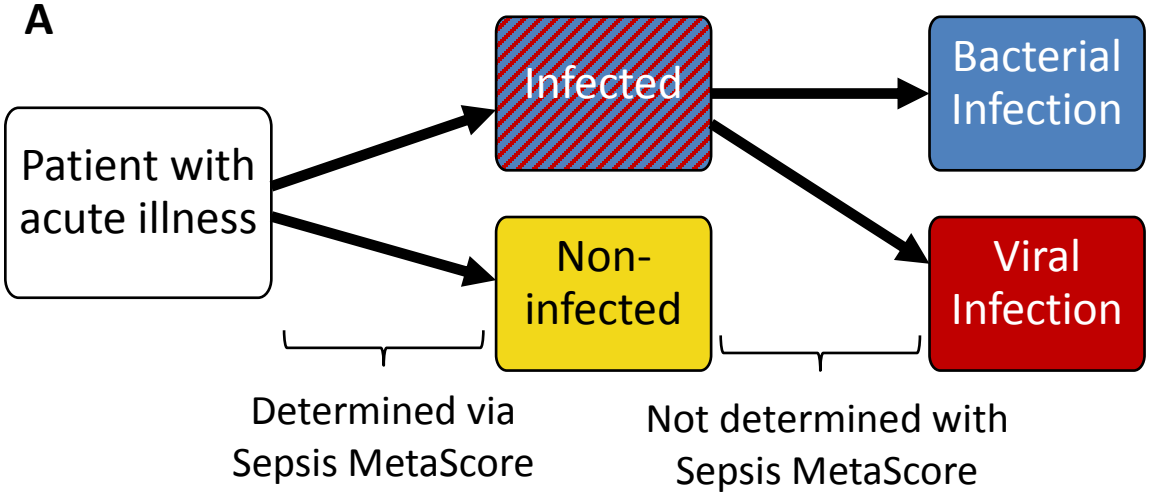

B	N bacterial	N viral	Mean SMS Bacterial	Mean SMS Viral	Wilcoxon W Statistic	Wilcoxon P value
EMEXP3589	4	5	0.372	-0.298	14	0.413
GSE15297	5	8	0.208	-0.13	21	0.943
GSE20346	12	8	-0.0292	0.0438	43	0.734
GSE25504 gpl13667	11	3	0.37	-1.36	32	**0.011**
GSE25504 gpl6947	26	1	0.0888	-2.31	26	0.0741
GSE40012	36	11	0.0348	-0.114	192	0.892
GSE40396	8	22	0.182	-0.0661	95	0.765
GSE42026	18	41	0.531	-0.233	536	**0.00537**
GSE60244	22	71	0.188	-0.0583	901	0.28
GSE63990	70	115	0.662	-0.403	6410	**1.59E-11**
GSE66099	109	11	0.0595	-0.59	792	0.0808

Supplementary Figure 1. The SMS and pathogen type. Diagram in (A) indicates how a decision model could be built. (B) Distribution of SMS in patients with bacterial vs. viral infections. Of 11 data sets, there were only three for which the SMS distribution showed a significant difference between bacterial and viral infections.

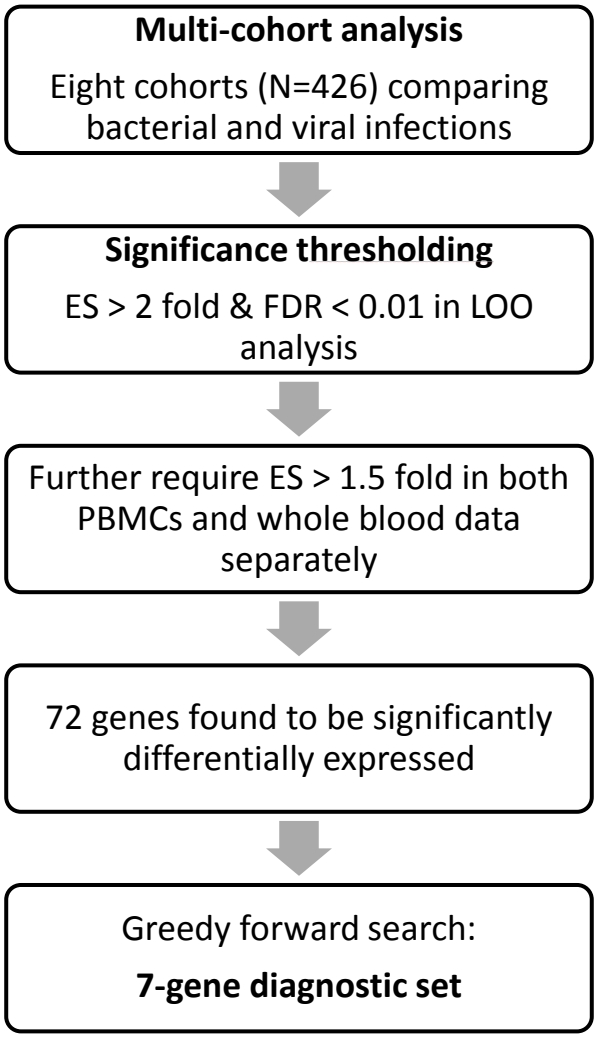

Supplementary Figure 2. Study schematic. Schematic of the workflow for the multi-cohort analysis and discovery of the bacterial-viral metasignature.

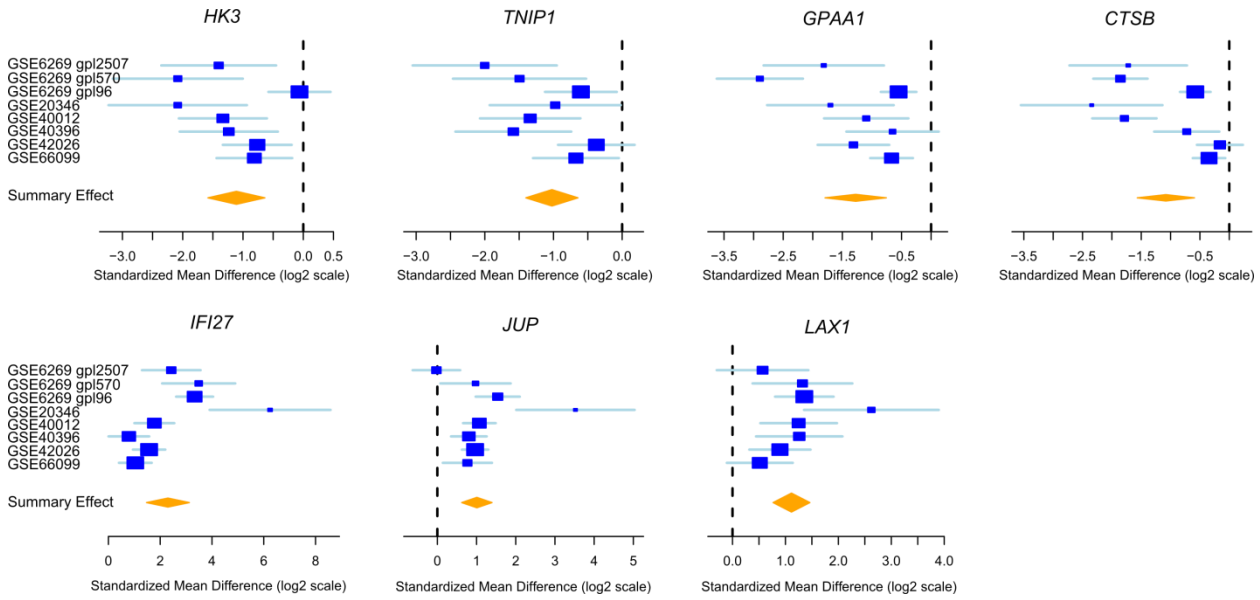

Supplementary Figure 3. Forest plots of the seven-gene set. Forest plots of the genes in the bacterial/viral metascore across the discovery data sets. The *x* axes represent standardized mean differences between bacterial and viral infection samples, computed as Hedges' *g*, in log2 scale. The size of the blue rectangles is inversely proportional to the standard error of the mean in the study. Whiskers represent the 95% confidence interval. The orange diamonds represent overall, combined mean difference for a given gene. Width of the diamonds represents the 95% confidence interval of overall combined mean difference.

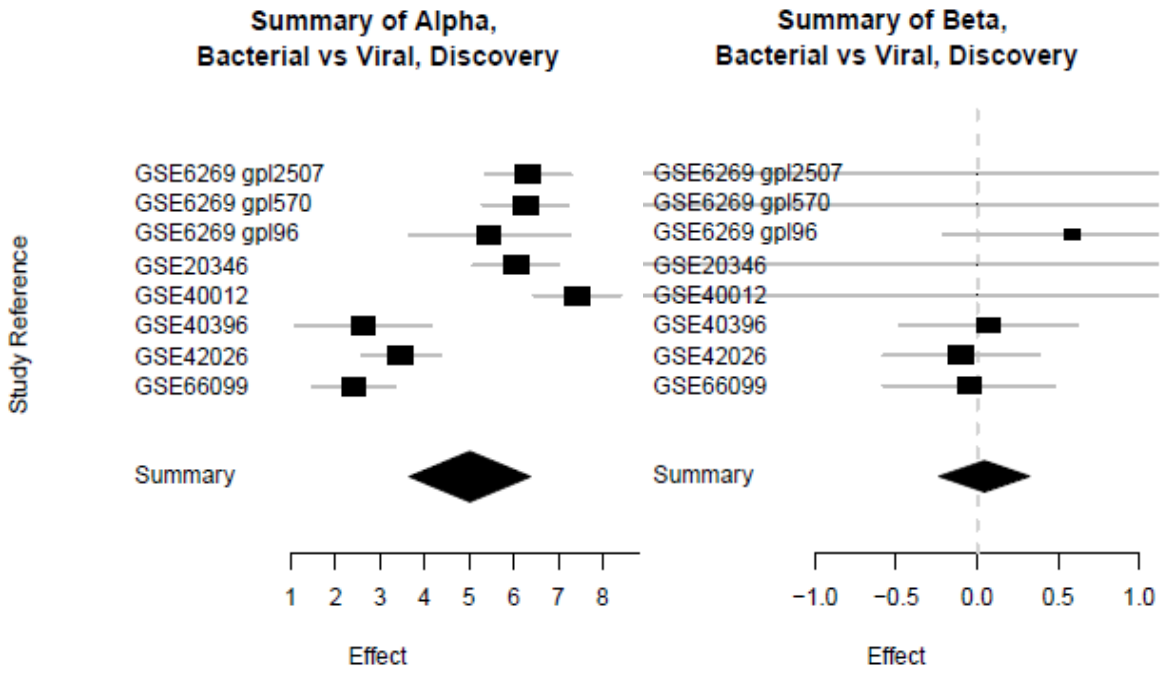

Supplementary Figure 4. Summary ROC forest plots for discovery data. Forest plots of the random-effects meta-analysis of the summary ROC parameters alpha and beta for the discovery data sets. Alpha roughly represents the distance from the line of identity (higher alpha = higher AUC) and beta represents the skew of the actual ROC curve [beta = 0 means no skew, and thus mirrored around the line from (1,0) to (0,1)].

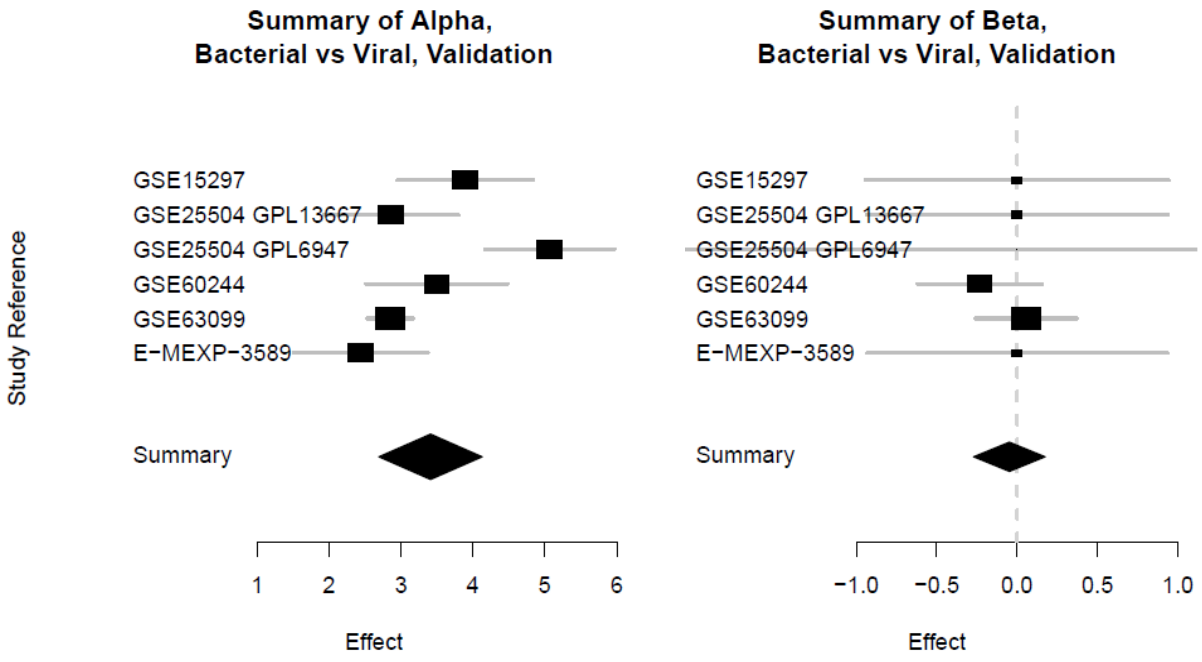

Supplementary Figure 5. Summary ROC forest plots for direct validation data. Forest plots of the random-effects meta-analysis of the summary ROC parameters alpha and beta for the validation data sets. Alpha roughly represents the distance from the line of identity (higher alpha = higher AUC) and beta represents the skew of the actual ROC curve [beta = 0 means no skew, and thus mirrored around the line from (1,0) to (0,1)].

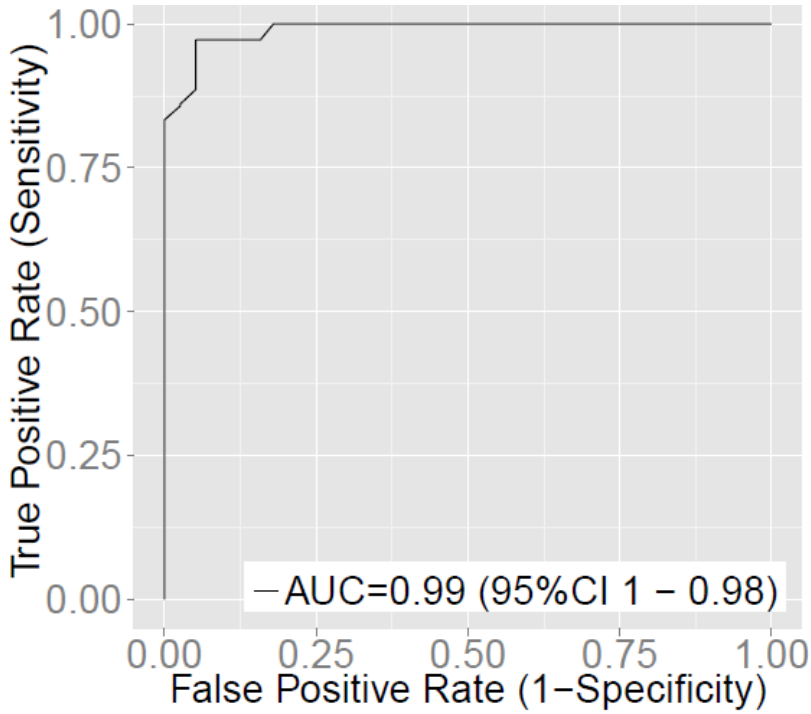

Supplementary Figure 6. Bacterial/viral metascore ROC in GSE53166. GSE53166 studied monocyte-derived dendritic cells stimulated in vitro with LPS or influenza virus, total N = 75 (39 LPS, 36 influenza virus).

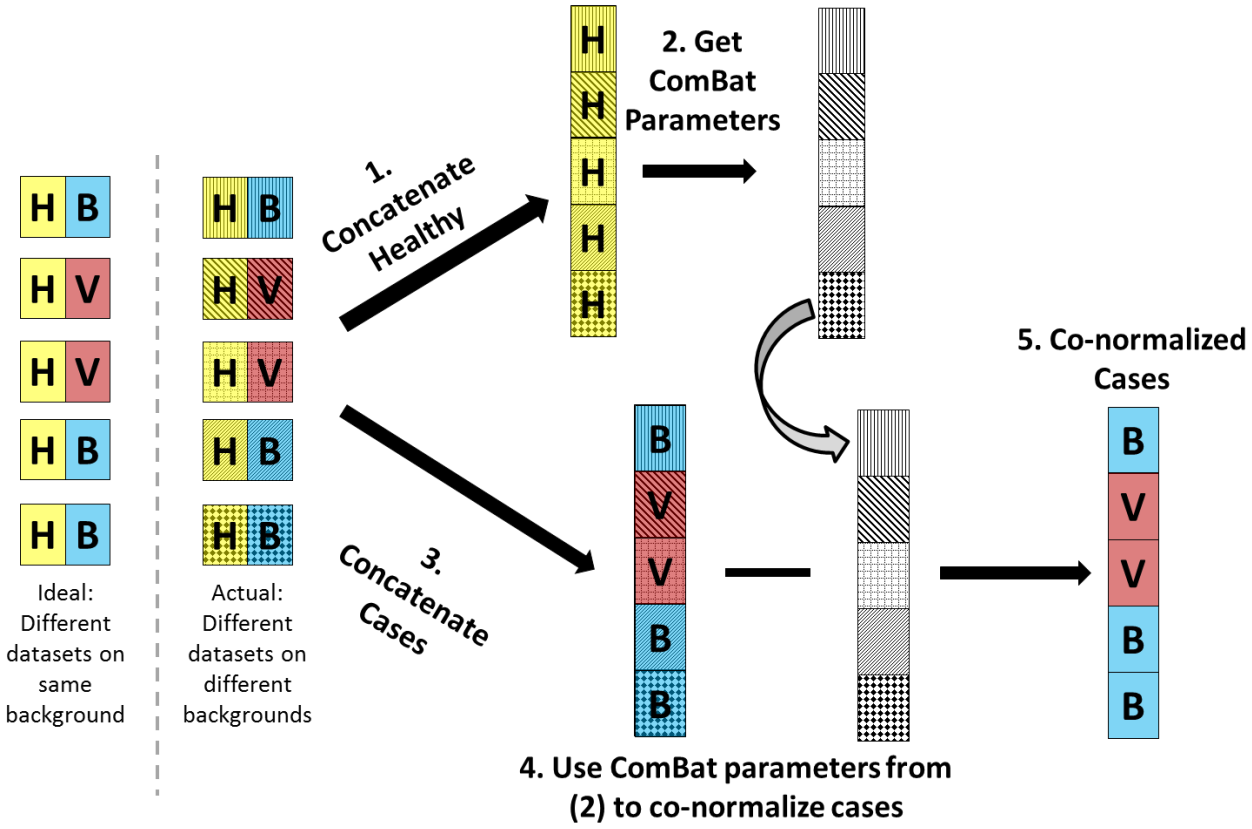

Supplementary Figure 7. Schematic of COCONUT conormalization. Yellow indicates healthy ('H'), red means viral ('V'), and blue means bacterial ('B'). Different crosshatchings are meant to indicate different batch effects. See Materials and Methods for formal mathematical details.

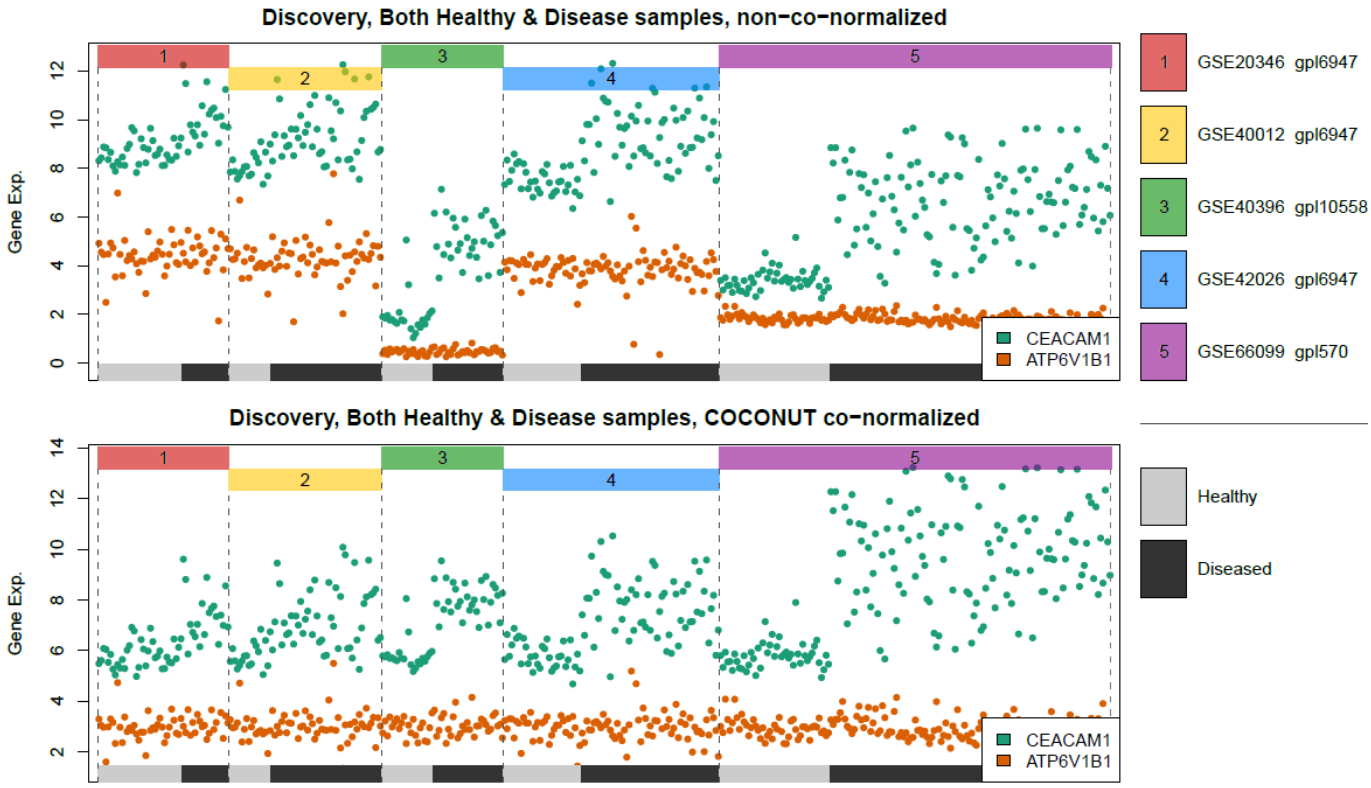

Supplementary Figure 8. COCONUT conormalization of whole-blood discovery data sets. Upper panel: raw data. Lower panel: COCONUT conormalized data. COCONUT conormalization resets each gene to be at the same location and scale for control patients. Distribution of a gene within a data set is unchanged [median difference in T-statistics for healthy vs. disease within data sets is 0, range (-1e-13, 1e-13), across all genes and all data sets]. Housekeeping genes (*ATP6V1B1*) exhibit expected invariance with respect to disease. Genes expected to be induced by infection (*CEACAM1*) exhibit baseline invariance (no change between data sets over gray bars), but can vary in disease states between data sets (variously induced between data sets over black bars). Upper color bars indicate data sets. Lower color bars indicate disease class (healthy vs. infected/diseased state).

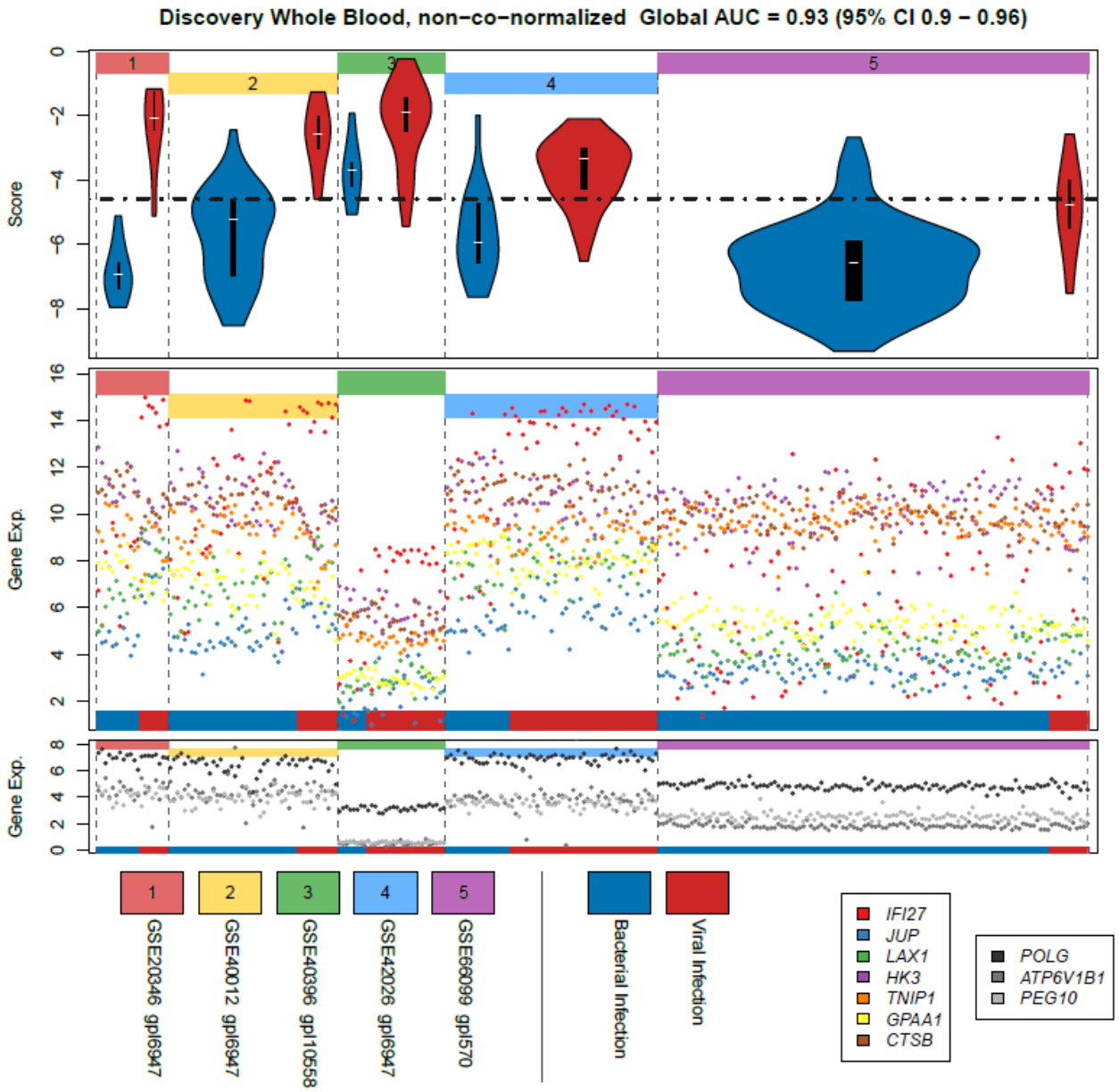

Supplementary Figure 9. Bacterial/viral score in global ROC of non-conormalized whole-blood discovery data sets. The global AUC across all whole-blood discovery data sets is 0.93. Upper panel: score distribution by data set (blue = bacterial, red = viral). Middle panel: individual gene expression levels. Lower panel: housekeeping genes (grayscale). Note the highly varying locations and scales of the housekeeping genes. The dotted line in the upper panel shows a possible global threshold for discriminating infection type.

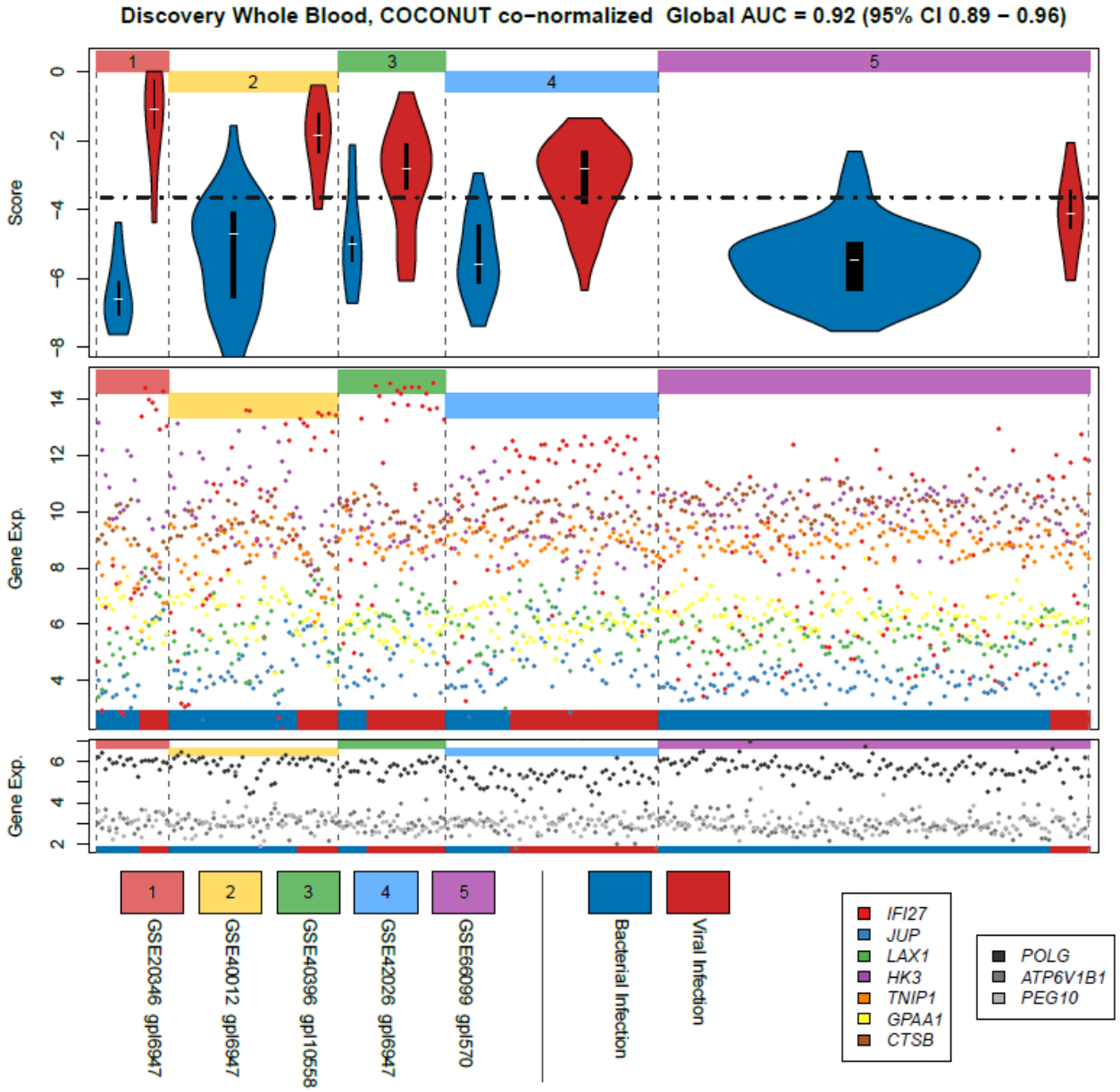

Supplementary Figure 10. Bacterial/viral score in global ROC of COCONUT-conormalized whole-blood discovery data sets. The global AUC across all whole-blood discovery data sets is 0.92. Upper panel: score distribution by data set (blue = bacterial, red = viral). Middle panel: individual gene expression levels. Lower panel: housekeeping genes (grayscale). The dotted line in the upper panel shows a possible global threshold for discriminating infection type.

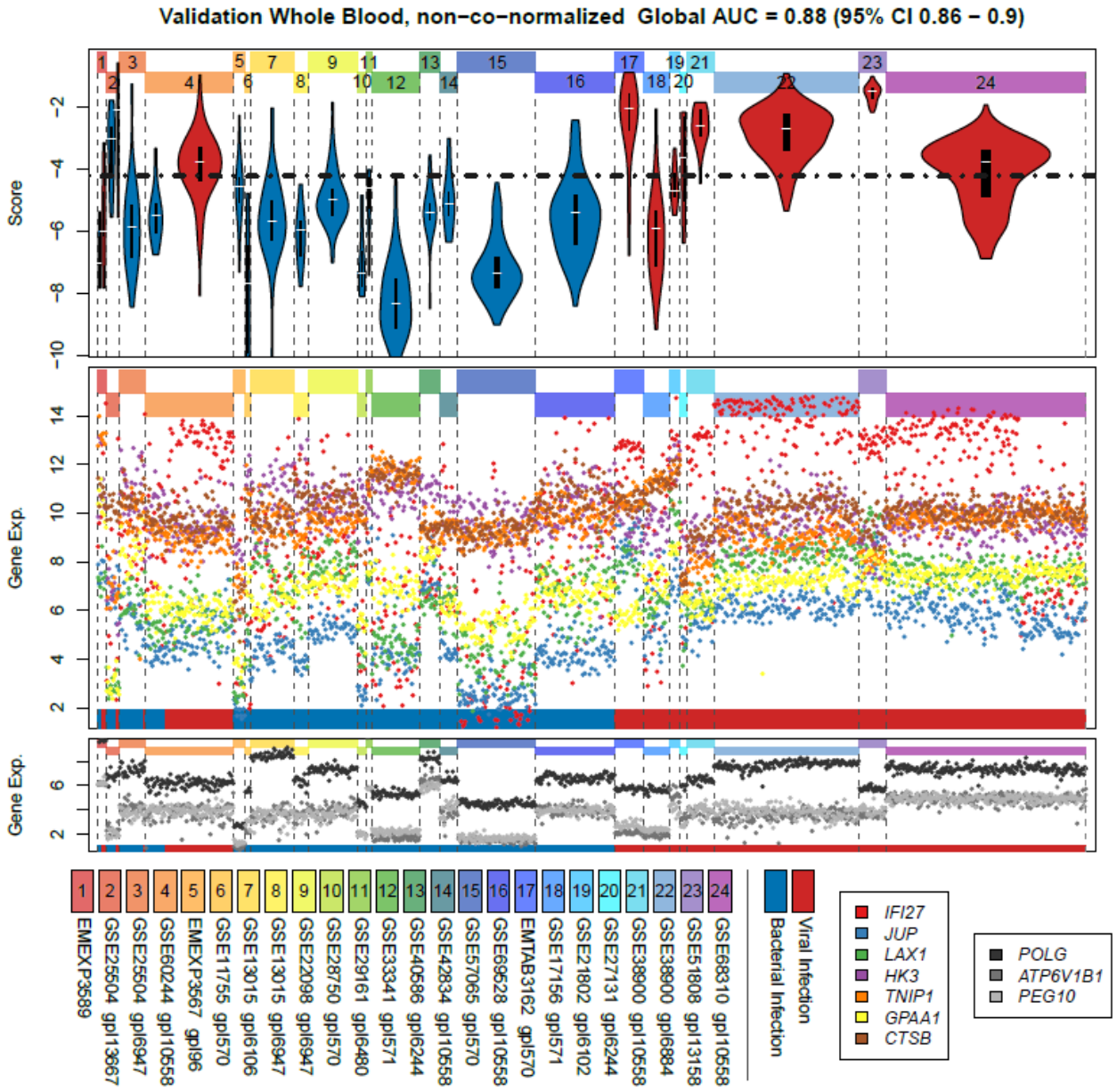

Supplementary Figure 11. Bacterial/viral score in global ROC of non-conormalized whole-blood validation data sets. Upper panel: score distribution by data set (blue = bacterial, red = viral). Middle panel: individual gene expression levels. Lower panel: housekeeping genes (grayscale). Note the highly varying locations and scales of the housekeeping genes. The dotted line in the upper panel shows a possible global threshold for discriminating infection type.

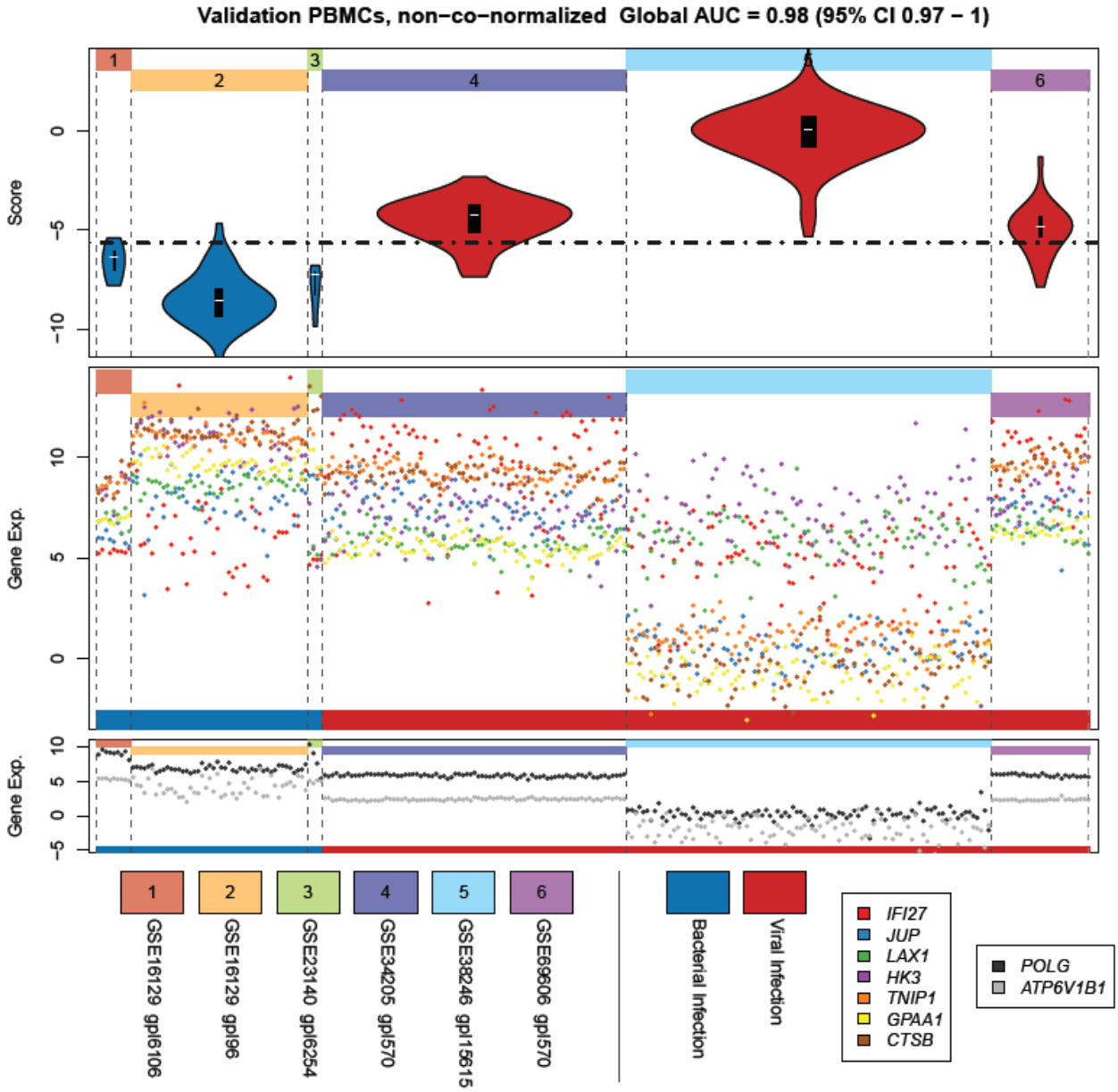

Supplementary Figure 12. Bacterial/viral score in global ROC of non-conormalized PBMC validation data sets. Upper panel: score distribution by data set (blue = bacterial, red = viral). Middle panel: individual gene expression levels. Lower panel: housekeeping genes (grayscale). Note the highly varying locations and scales of the housekeeping genes. The dotted line in the upper panel shows a possible global threshold for discriminating infection type.

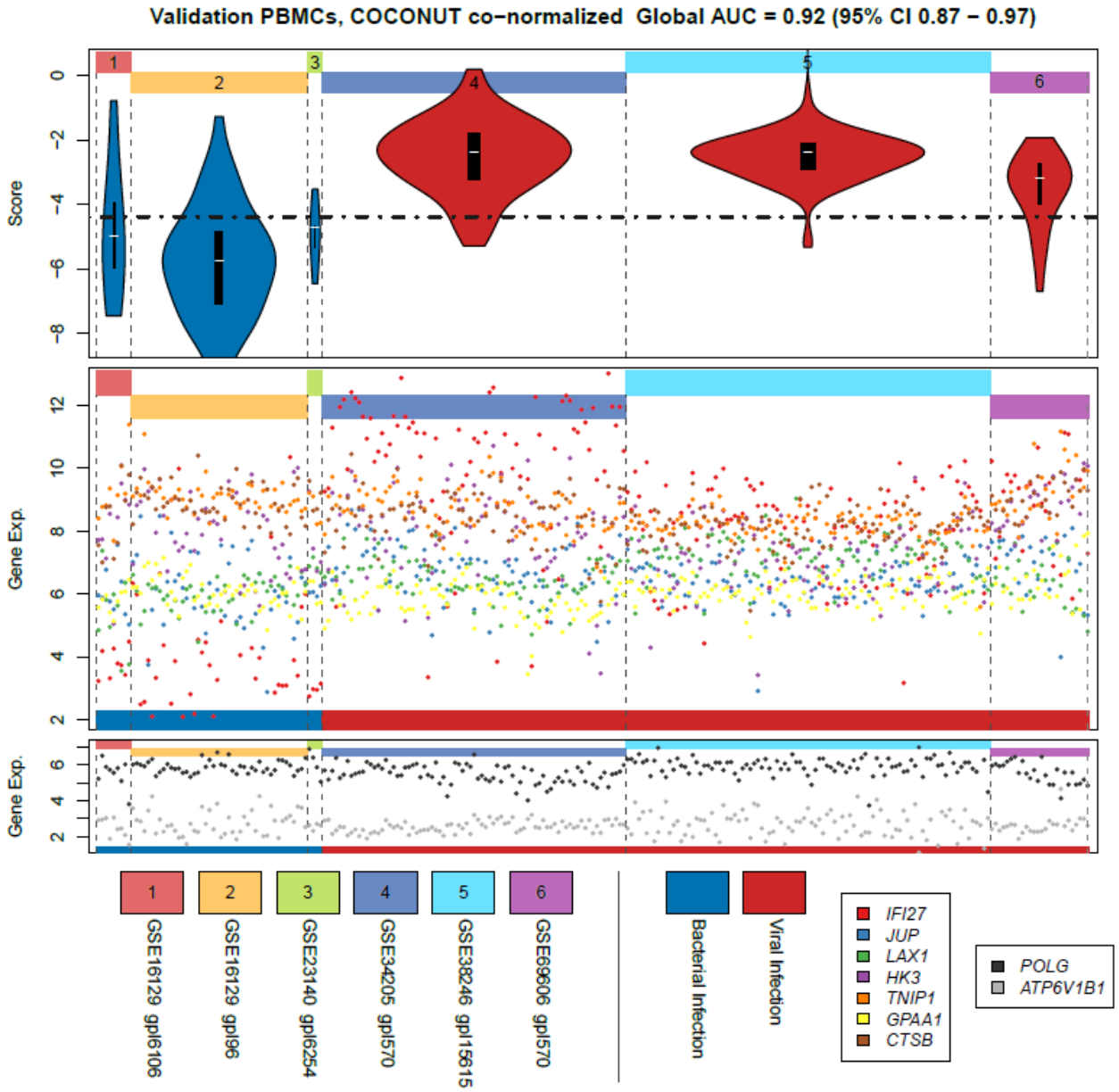

Supplementary Figure 13. Bacterial/viral score in global ROC of COCONUT-conormalized PBMC validation data sets. The global AUC across all PBMC validation data sets is 0.92. Upper panel: score distribution by data set (blue = bacterial, red = viral). Middle panel: individual gene expression levels. Lower panel: housekeeping genes (grayscale). The dotted line in the upper panel shows a possible global threshold for discriminating infection type.

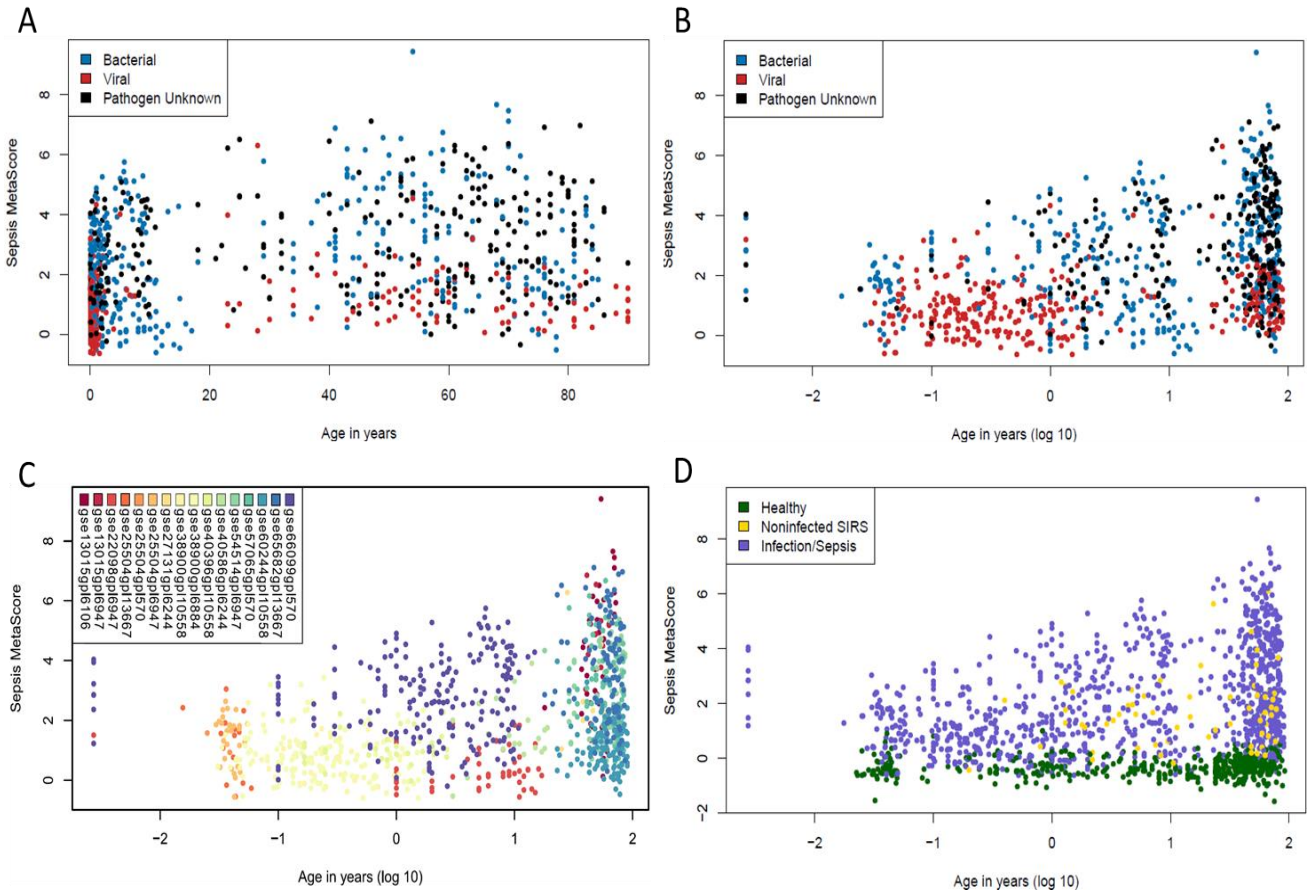

Supplementary Figure 14. The effects of age on SMS in COCONUT-conormalized data. (A) Age vs. SMS by pathogen type. (B) Log10(age) vs. SMS by pathogen type. (C) Log10(age) vs. SMS by data set. A-C only include infected patient samples. (D) Log10(age) vs. SMS shows both healthy and non-infected SIRS samples in addition to acute infections. In all cases, the GSE25504 age data are randomly distributed according to the mean age given in their manuscript, roughly 2 weeks +/- 1 week because individual ages are not available. All ages=0 were reset as age=1/365.

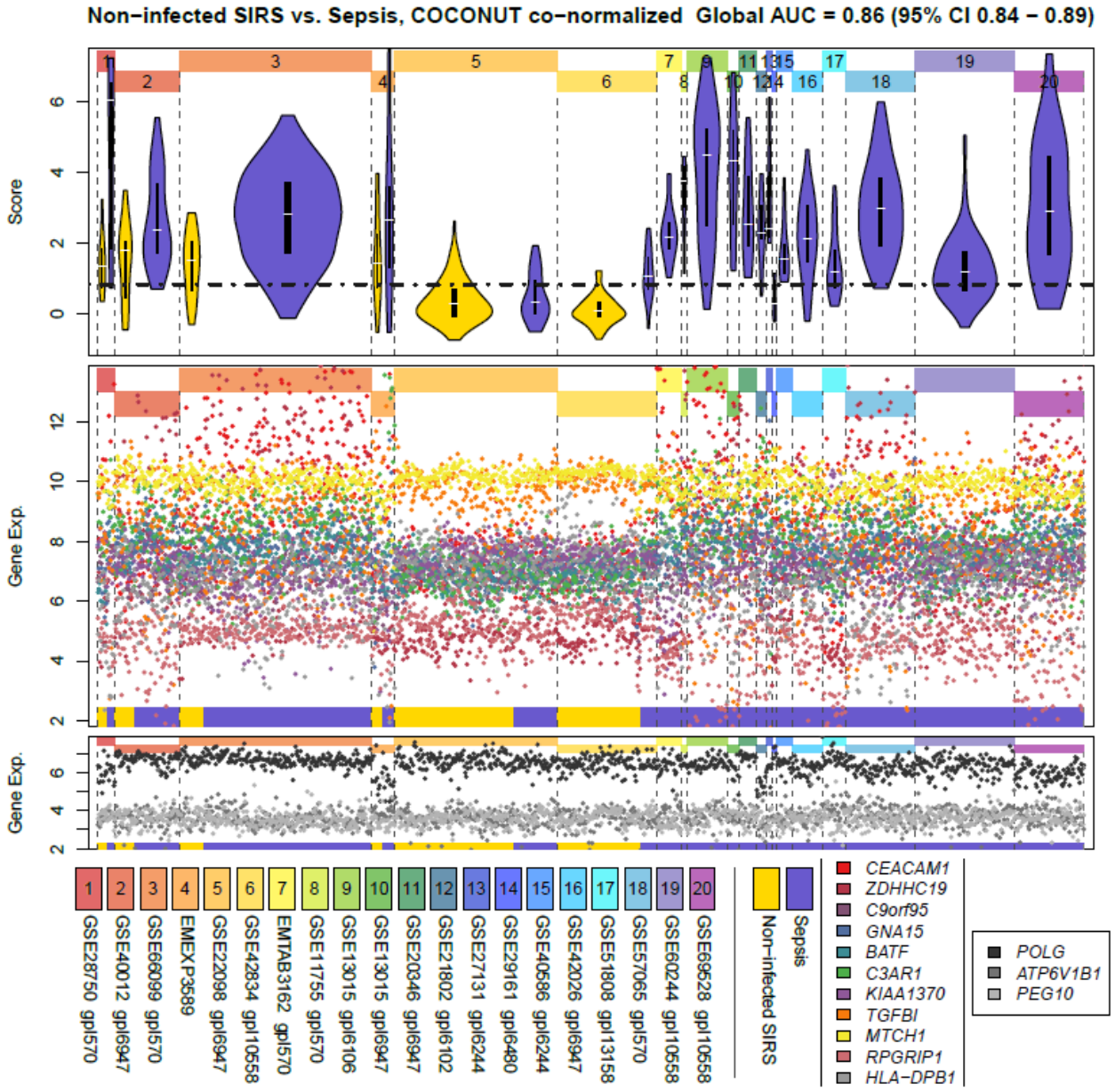

Supplementary Figure 15. SMS across all COCONUT-conormalized whole-blood data (both discovery and validation). The global AUC is 0.86 (95% CI 0.84-0.89). Upper panel: score distribution by data set (yellow = non-infected inflammation, purple = infections/sepsis). Middle panel: individual gene expression levels. Lower panel: housekeeping genes (grayscale). The dotted line in the upper panel shows a possible global threshold for discriminating infections.

A

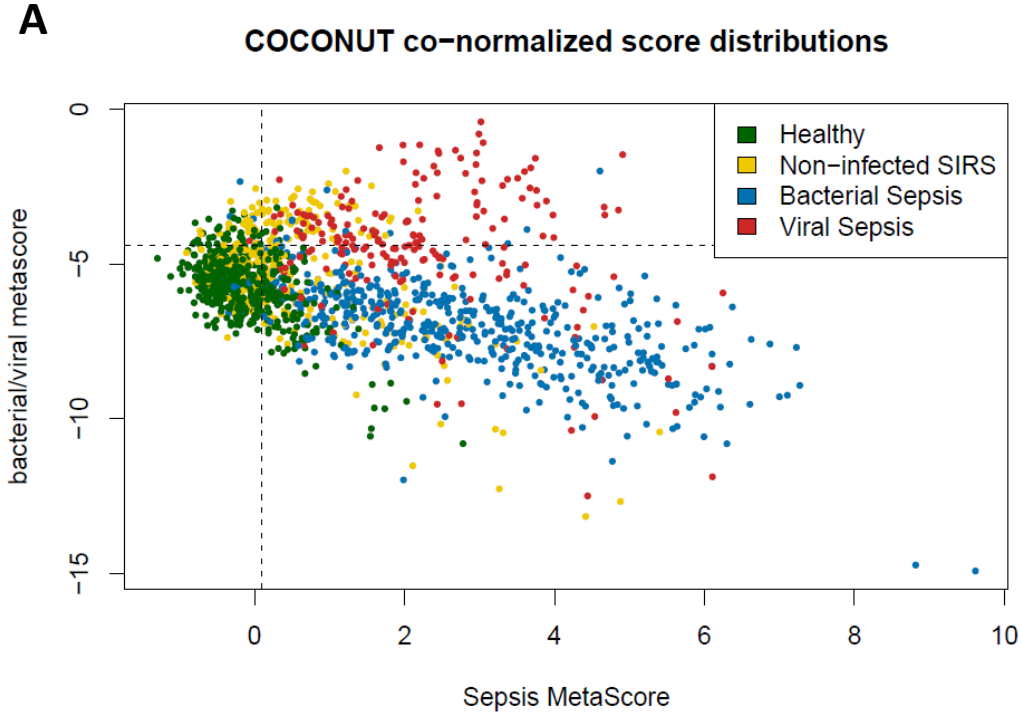

B		Predicted		
		Healthy & SIRS	bacterial	viral
Ground Truth	Healthy & SIRS	560	245	72
	bacterial	19	505	12
	viral	1	94	107

Supplementary Figure 16. IADM across COCONUT-conormalized public gene expression data including healthy controls. The included data sets and the score cutoffs used are the same as those in Figure 3. (A) Distribution of scores for IADM in COCONUT-conormalized data. (B) Confusion matrix for diagnosis. Bacterial infection sensitivity: 94.2%; bacterial infection specificity: 68.5%; viral infection sensitivity: 53.0%; viral infection specificity: 94.1%. 'SIRS' refers to non-infected inflammation.

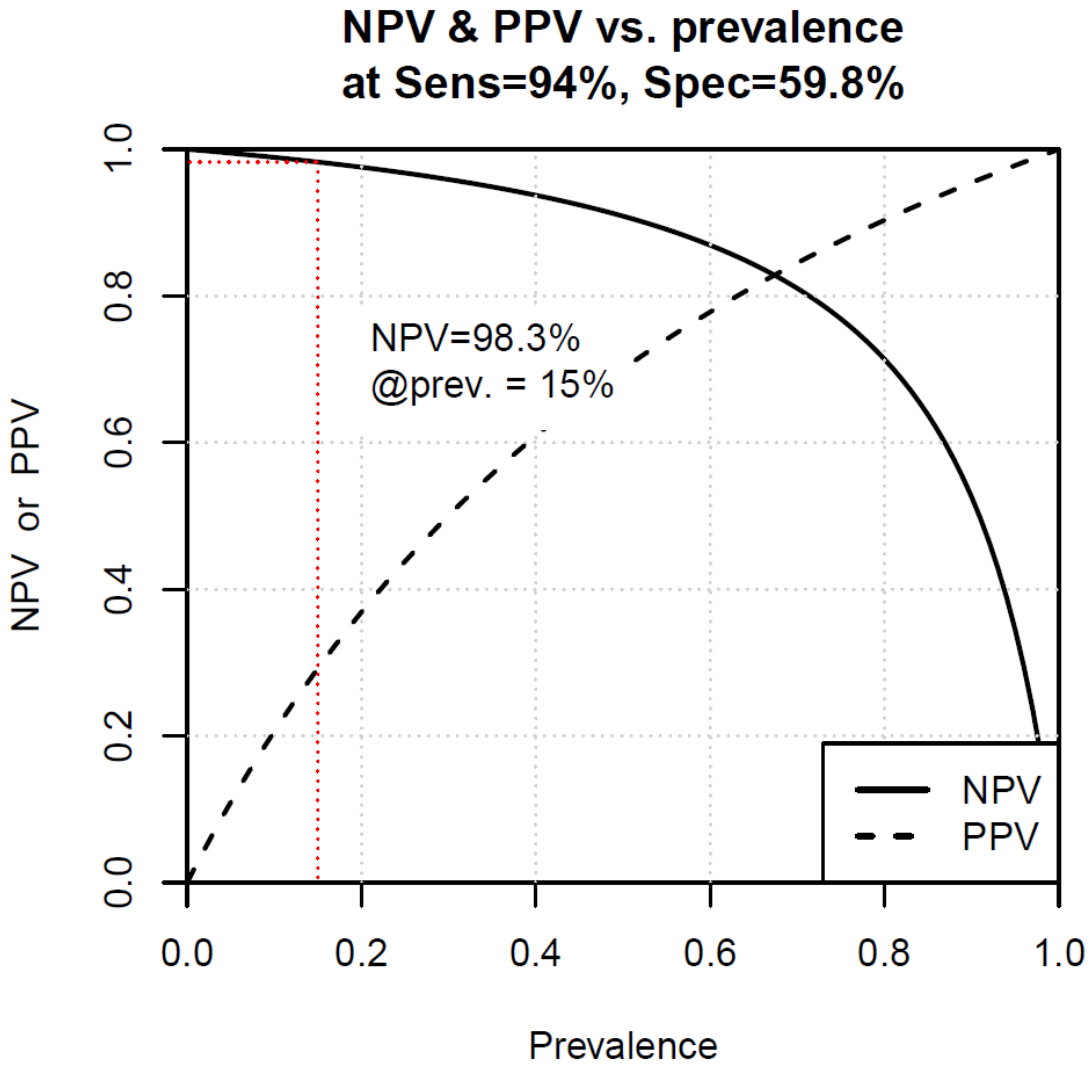

Supplementary Figure 17. NPV and PPV for the IADM. NPV and PPV vs. prevalence for a diagnostic test with 94.0% sensitivity and 59.8% specificity. Red lines show an NPV of 98.3% at a prevalence of 15%, as a rough estimate for real case-rates of infection.

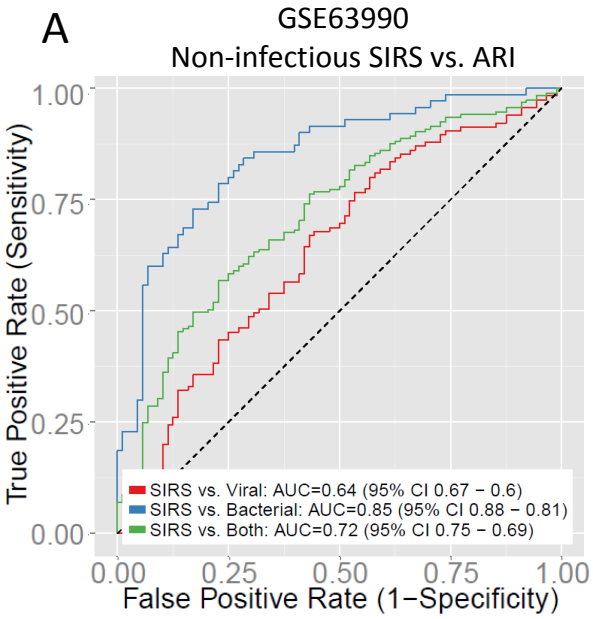

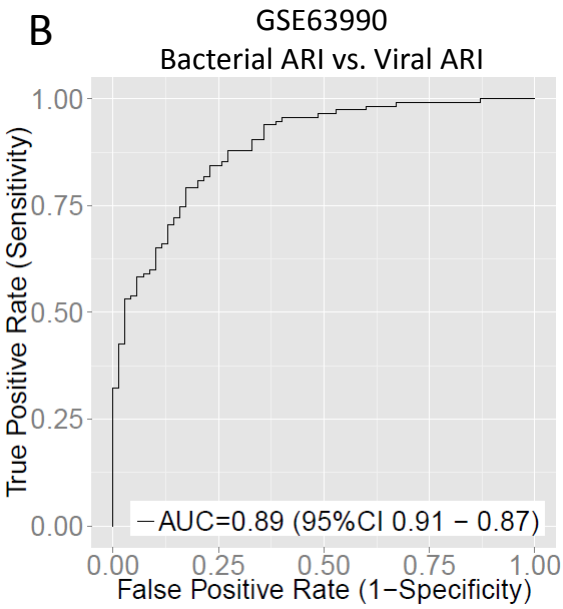

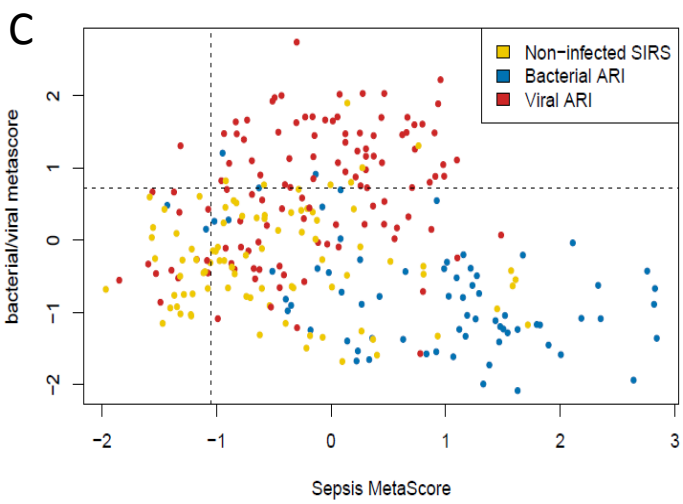

D

		Predicted		
		sterile SIRS	bact	viral
Ground Truth	sterile SIRS	25	56	7
	bact	2	66	2
	viral	14	41	60

Supplementary Figure 18. GSE63990, adults with ARIs. (A and B) ROC curves for the Sepsis MetaScore and the bacterial/viral metascore. (C), Distribution of scores and cutoffs for IADM. (D) Confusion matrix for IADM. Bacterial infection sensitivity: 94.3%; bacterial infection specificity: 52.2%; viral infection sensitivity: 52.2%; viral infection specificity: 94.3%.

	summary effect size	summary effect size std.err.	tau^2	hetero-geneity p value	Q	df	overall p value	overall FDR (q value)	mean discovery weighted AUC
OAS1	1.184	0.146	0.105	0.003	21.322	7	4.56E-16	5.43E-12	0.808
IFIT1	1.422	0.203	0.192	0.007	19.389	7	2.47E-12	4.42E-09	0.826
TSPO	-1.233	0.177	0.141	0.009	18.858	7	3.42E-12	5.79E-09	0.781
SAMD9	1.063	0.155	0.072	0.121	11.416	7	7.30E-12	9.66E-09	0.752
EMR1	-1.074	0.158	0.054	0.206	9.705	7	9.39E-12	1.12E-08	0.768
ISG15	1.625	0.242	0.278	0.008	19.227	7	1.79E-11	1.93E-08	0.829
HERC5	1.361	0.207	0.178	0.032	15.336	7	4.58E-11	3.89E-08	0.794
NINJ2	-1.008	0.154	0.048	0.223	9.434	7	5.75E-11	4.67E-08	0.741
DDX60	1.303	0.200	0.159	0.042	14.565	7	6.91E-11	5.25E-08	0.797
HESX1	1.107	0.172	0.091	0.116	11.549	7	1.28E-10	8.69E-08	0.749
IFI6	1.292	0.204	0.199	0.005	20.207	7	2.28E-10	1.33E-07	0.794
MX1	1.600	0.253	0.328	0.003	21.525	7	2.63E-10	1.49E-07	0.826
OASL	1.192	0.189	0.195	0.001	25.432	7	2.73E-10	1.52E-07	0.788
LAX1	1.114	0.178	0.103	0.097	12.125	7	3.59E-10	1.86E-07	0.769
ACPP	-1.143	0.183	0.135	0.035	15.099	7	4.41E-10	2.19E-07	0.777
TBXAS1	-1.213	0.195	0.159	0.031	15.409	7	5.43E-10	2.55E-07	0.765
IFIT5	1.076	0.174	0.126	0.027	15.825	7	6.47E-10	3.00E-07	0.760
IFIT3	1.331	0.216	0.269	0.000	32.727	7	7.55E-10	3.42E-07	0.794
KCTD14	1.163	0.190	0.161	0.011	18.106	7	8.80E-10	3.83E-07	0.739
OAS2	1.379	0.230	0.346	0.000	56.480	7	1.99E-09	7.33E-07	0.830
PGD	-1.121	0.189	0.130	0.062	13.439	7	2.95E-09	1.01E-06	0.752
RTP4	1.084	0.189	0.132	0.059	13.565	7	9.15E-09	2.68E-06	0.741
PARP12	1.189	0.208	0.193	0.021	16.436	7	1.12E-08	3.13E-06	0.769
LY6E	1.479	0.260	0.363	0.001	23.586	7	1.29E-08	3.48E-06	0.818
S100A12	-1.067	0.190	0.135	0.056	13.727	7	1.81E-08	4.58E-06	0.737
ADA	1.015	0.183	0.146	0.015	17.395	7	2.79E-08	6.47E-06	0.730
IFI44L	1.727	0.311	0.568	0.000	31.320	7	2.90E-08	6.63E-06	0.823
SORT1	-1.013	0.184	0.161	0.005	20.064	7	4.00E-08	8.89E-06	0.760
IFI27	2.299	0.423	1.147	0.000	50.156	7	5.67E-08	1.16E-05	0.867
RSAD2	1.573	0.292	0.528	0.000	35.451	7	7.48E-08	1.47E-05	0.825
IFI44	1.519	0.283	0.493	0.000	37.895	7	8.24E-08	1.57E-05	0.816
OAS3	1.285	0.240	0.344	0.000	33.835	7	9.09E-08	1.69E-05	0.808
IFIH1	1.014	0.192	0.183	0.003	21.908	7	1.36E-07	2.42E-05	0.788
TNIP1	-1.023	0.194	0.152	0.040	14.735	7	1.42E-07	2.50E-05	0.749
RAB31	-1.167	0.225	0.284	0.000	31.645	7	2.27E-07	3.70E-05	0.753
SIGLEC1	1.447	0.281	0.493	0.000	38.460	7	2.59E-07	4.13E-05	0.816
SLC12A9	-1.215	0.237	0.306	0.000	27.836	7	2.87E-07	4.43E-05	0.786

JUP	1.008	0.198	0.209	0.000	26.258	7	3.66E-07	5.40E-05	0.783
STAT1	1.009	0.199	0.260	0.000	59.749	7	3.78E-07	5.51E-05	0.739
CUL1	1.060	0.212	0.225	0.004	20.680	7	5.96E-07	7.91E-05	0.753
PLP2	-1.246	0.250	0.325	0.002	22.620	7	5.99E-07	7.92E-05	0.768
IMPA2	-1.428	0.290	0.485	0.000	29.554	7	8.28E-07	0.0001016	0.778
DNMT1	1.071	0.217	0.222	0.012	18.048	7	8.34E-07	0.0001016	0.741
IFIT2	1.103	0.226	0.273	0.001	23.533	7	1.01E-06	0.0001183	0.749
GPAA1	-1.275	0.265	0.432	0.000	43.119	7	1.50E-06	0.0001581	0.775
CHST12	1.177	0.246	0.342	0.000	27.608	7	1.62E-06	0.0001679	0.772
LTA4H	-1.585	0.332	0.666	0.000	36.759	7	1.76E-06	0.0007814	0.766
RTN3	-1.045	0.221	0.307	0.000	46.192	7	2.39E-06	0.0002217	0.757
CETP	-1.132	0.242	0.333	0.000	29.766	7	2.86E-06	0.0002558	0.728
ISG20	1.214	0.262	0.411	0.000	34.693	7	3.64E-06	0.0003074	0.758
TALDO1	-1.138	0.246	0.344	0.000	30.764	7	3.66E-06	0.0003084	0.737
DHX58	1.197	0.259	0.370	0.001	24.871	7	3.94E-06	0.0003259	0.732
EIF2AK2	1.347	0.293	0.554	0.000	47.713	7	4.28E-06	0.0003486	0.796
HK3	-1.109	0.242	0.304	0.002	22.157	7	4.53E-06	0.0003631	0.748
ACAA1	-1.077	0.235	0.309	0.000	28.834	7	4.61E-06	0.0003681	0.745
XAF1	1.300	0.288	0.552	0.000	55.144	7	6.56E-06	0.0004871	0.782
GZMB	1.203	0.267	0.394	0.000	26.203	7	6.72E-06	0.0004952	0.770
CAT	-1.034	0.230	0.322	0.000	43.416	7	6.86E-06	0.0005017	0.710
DOK3	-1.035	0.233	0.295	0.001	25.110	7	9.08E-06	0.0006200	0.709
SORL1	-1.213	0.273	0.487	0.000	56.464	7	9.12E-06	0.0006216	0.777
PYGL	-1.157	0.261	0.375	0.001	25.452	7	9.46E-06	0.0006406	0.754
DYSF	-1.127	0.256	0.359	0.001	24.813	7	1.09E-05	0.0007144	0.748
TWF2	-1.081	0.248	0.326	0.002	23.101	7	1.27E-05	0.0007883	0.736
TKT	-1.155	0.266	0.434	0.000	40.903	7	1.40E-05	0.000852	0.728
CTSB	-1.080	0.249	0.403	0.000	64.209	7	1.48E-05	0.0008831	0.695
FLII	-1.159	0.271	0.461	0.000	46.721	7	1.95E-05	0.0011014	0.716
PROS1	-1.250	0.296	0.520	0.000	31.989	7	2.37E-05	0.0012745	0.708
NRD1	-1.103	0.261	0.400	0.000	31.123	7	2.40E-05	0.0012827	0.730
STAT5B	-1.013	0.240	0.343	0.000	44.775	7	2.46E-05	0.0013136	0.736
CYBRD1	-1.022	0.242	0.357	0.000	36.401	7	2.48E-05	0.0013183	0.715
PTAFR	-1.083	0.257	0.403	0.000	39.437	7	2.55E-05	0.0013482	0.727
LAPTM5	-1.010	0.243	0.341	0.000	31.034	7	3.32E-05	0.0016574	0.718

Supplementary Table 1. Significant gene list. List of all genes found to be significant (q<0.01, ES>2 fold overall, and ES >1.5 fold in both PBMCs and whole blood separately) in multi-cohort analysis.

	sensitivity	specificity	true positives	true negatives	false positives	false negatives
GSE15297	0.875	1	7	5	0	1
GSE25504 GPL13667	1	0.818	3	9	2	0
GSE25504 GPL6947	1	1	1	26	0	0
GSE60244	0.944	0.636	67	14	8	4
GSE63990	0.948	0.614	109	43	27	6
E-MEXP-3589	1	0.75	5	3	1	0

Supplementary Table 2. Test characteristics of the bacterial/viral metascore in direct validation data sets.

Accession	Non-infected condition	Infected condition	Number Healthy	Number Non-Infected	Number Infected
GSE28750	Post-surgical adults	Adults with community-acquired bacterial sepsis	20	11	10
GSE40012	Non-infected SIRS in adult ICU	Adults with CAP in ICU	18	24	47
GSE66099	Non-infected SIRS in pediatric ICU	Pediatric sepsis, severe sepsis and septic shock	47	30	120
E-MEXP-3589	Non-infected hospitalized patients with COPD	Hospitalized patients with COPD with respiratory infections	4	14	9
GSE22098	Children and adults with SLE and Still's disease	Children with Gram positive infections	81	141	52
GSE42834	Adults with sarcoidosis and lung cancer	Adults with bacterial pneumonia	118	99	19

Supplementary Table 3. Data sets with noninfected inflammatory conditions used to test the IADM. Other data sets are listed in Tables 1 & 2. ICU: intensive care unit. CAP: community-acquired pneumonia. SLE: systemic lupus erythematosus.

Supplementary Table 4. NanoString data (provided as a separate spreadsheet). Normalized, log2-transformed NanoString nCounter data for all genes in the IADM for the 96-patient pediatric validation cohort.

Supplementary Acknowledgements. The authors would like to thank the following 382 authors of the papers describing the data sets used in this manuscript. In this era of open data sharing, proper credit to the data generators is paramount.

Ahmed R, Ahn SH, Ahout IM, Aldunate S, Allantaz F, Allen GL, Allman W, Almansa R, Amara AB, Anas N, Andaluz-Ojeda D, Andaluz D, Andeweg A, Andeweg AC, Anfasa F, Antón A, Arden N, Ardura M, Ardura MI, Armstrong NJ, Aronow BJ, Atmar RL, Aukrust P, Balmaseda A, Banchereau J, Banchereau JF, Banchereau R, Bancroft GJ, Banner D, Banschbach S, Barbado J, Barnes M, Beckman E, Belmont JW, Benoist CO, Berdal JE, Bermejo-Martin JF, Berry MP, Beynon H, Bigham MT, Bijl MA, Blanco J, Blankenship DM, Blankley S, Bloch SA, Bloom CI, Bobillo F, Booth DR, Bouvry D, Brand HK, Brandon RA, Brandon RB, Bucasas KL, Buddhisa S, Bunsow E, Burke T, Burns JC, Cairns CB, Capo C, Carin L, Carrol ED, Castro C, Cazalis MA, Chan S, Chaussabel D, Checchia PA, Chen L, Chen M, Chipendo PI, Chokephaibulkit K, Chopra A, Chung W, Conejero L, Couch RB, Craigon M, Crosby SD, Cush JJ, Cvijanovich NZ, Cyr DD, Day PJ, de Groot R, De Jager PL, de Lejarazu RO, de Ridder D, del Olmo M, Denis B, Devouassoux G, Dewi BE, Dhawan R, Di Pucchio T, Dickinson P, Dimo B, Disdier C, Doctor A, Dominique V, Dunsmore K, Durbin JE, Eisenhaure TM, Emonts M, Falsey AR, Fernandes C, Fernandez V, Ferry T, Ferwerda G, Filali AE, Fink C, Flanagan KL, Flaño E, Forster T, Fowler VG, Frager F, France R, Franco LM, Freeman DH, Freishtat RJ, Frohlich IY, Furuseth MT, Gallegos MC, Gandía F, Garcia C, Ghazal P, Gilbert A, Ginsburg GS, Glaser C, Glickman SW, Gómez-Sánchez MJ, Gordon A, Gordón M, Gormley S, Gorochov G, Graham CM, Guiver M, Habib G, Hacohen N, Hafler DA, Hall M, Halvorsen B, Harmon K, Harris E, Henao R, Henricksen JW, Herberg JA, Hermans PW, Hero AO, Herrero A, Ho LP, Hu X, Huang S, Huang SJ, Huang Y, Hudson LL, Iglesias V, Imboywa SH, Ioannidis I, Irwin AD, Ivens A, Jackson A, Jaehne AK, Jartti T, Jeffers G, Jonassen CM, Jones KD, Jordan-Villegas A, Kaforou M, Kalyanaraman M, Kanegaye JT, Kaur R, Kellis M, Kelvin D, Kendrick Y, Khaenam P, Khondoker MR, Kingsmore SF, Kjekshus H, Ko ER, Kõks S, Kolamunnage-Dona R, Kon OM, Kwissa M, Laake JH, Lacaze P, Lahni P, Lambkin-Williams R, Langley RJ, Lee MH, Lee MN, León C, Lepape A, Lertmemongkolchai G, Levin M, Li W, Li Y, Lill M, Lin R, Lipman J, Lipman M, Liu K, Liu M, Lopez-Campos G, Loza A, Lucas J, Lutsar I, Lynn DJ, Maagaard A, Manak J, Mankhambo LA, Maravi E, Marcos M, Marriage F, Martín-Loeches I, Martin-Sanchez F, Martina BE, Martinon-Torres F, Mazur A, McCabe C, McClain MT, McLean AS, McNab FW, McNally B, Mege JL, Mejias A, Merino P, Meyer K, Miyara M, Mollnes TE, Molyneux EM, Molyneux ME, Monaco M, Monneret G, Montana G, Mougin B, Nainggolan L, Nakaya HI, Nalos M, Ng DC, Nguyen T, Nichols M, Nicholson B, Niño D, Nogueira B, Nowak J, O'Garra A, Odoms K, Øien NC, Olstad OK, Oni T, Onlamoon N, Orme J, Ortiz de Lejarazu R, Osterhaus AD, Otero RM, Pachot A, Palucka AK, Pankla-Sranujit R, Pankla R, Parnell GP, Pascoe R, Pascual V, Patel S, Pattanapanyasat K, Paulus S, Paye M, Peeples ME, Penfil S, Perng GC, Pichichero M, Piqueras B, Popper SJ, Potempa K, Price G, Pulendran B, Pumarola T, Quackenbush EB, Quarles JM, Quasney M, Quinn C, Raddassi K, Raj T, Ramilo O, Ramirez P, Ran FA, Ran L, Raoult D, Raychaudhuri S, Redford PS, Regev A, Rello J, Relman DA, Resino S, Rico L, Rivers EP, Roeleveld N, Roig V, Rojo S, Rosich S, Ross A, Rozakeas F, Saadatian M, Sakthivel B, Salguero FJ, San-Jose CA, Sanchez-Garcia M, Schalkwyk LC, Sen A, Shanley TP,

Shaw CA, Shimizu C, Skinner J, Slowikowski K, Smith CL, Socias L, Soomets U, Spink N, Staal FJ, Stenson BJ, Stone G, Storch GA, Stranger BE, Study IG, Suarez-Arrabal MC, Suarez NM, Sumner ER, Sutherland A, Taba P, Tagavilla MA, Tam OY, Tang BM, Tang W, Textoris J, Thomas M, Thomas NJ, Thuny F, Tofil NM, Tsalik EL, Turner R, Ueland T, Valeyre D, Vallin H, van de Weg CA, van den Ham HJ, van Diepen A, van Gorp EC, van IJcken WF, van Velkinburgh JC, Vancheeswaran R, Vanhems P, Varillas D, Varkey J, Veldman T, Venet F, Venter D, Villani AC, Villinger F, Wæhre T, Walsh EE, Wang X, Wang Y, Ward LD, Warris A, Watson VE, Wells JM, Wickremasinghe M, Wilkinson KA, Wilkinson RJ, Willette M, Wittkowski KM, Wong HR, Woods CW, Wrammert J, Wright VJ, Xu L, Xu Z, Yu J, Ye C, Yoksan S, Zaalberg M, Zaaraoui-Boutahar F, Zaas AK, Zapata GE, Zhai Y, Zhang F, Zhang Y.